

1 **UNSUPERVISED DETECTION OF HARSH CORNERING BEHAVIOR USING**  
2 **SMARTPHONE-BASED TELEMATICS AND INFRASTRUCTURE DATA**

3

4

5

6 **Aristotelis Tsoutsanis, M.Sc. Ph.D Candidate, Corresponding Author**

7 Department of Transportation Planning and Engineering

8 National Technical University of Athens, Athens, Greece, 15772

9 OSeven Telematics

10 Chaimanta 27B, Athens, Greece, 15234

11 a\_tsoutsanis@mail.ntua.gr, atsoutsanis@oseven.io

12

13 **Apostolos Ziakopoulos, Ph.D**

14 Department of Transportation Planning and Engineering

15 National Technical University of Athens, Athens, Greece, 15772

16 apziak@central.ntua.gr

17

18 **Zoe Vasileiou, M.Sc.**

19 OSeven Telematics

20 Chaimanta 27B, Athens, Greece, 15234

21 zvasileiou@oseven.io

22

23 **George Yannis, Professor**

24 Department of Transportation Planning and Engineering

25 National Technical University of Athens, Athens, Greece, 15772

26 geyannis@central.ntua.gr

27

28

29 Word Count: 4480 words + 2 table(s) × 250 = 4980 words

30

31

32

33

34

35

36 Submission Date: January 8, 2026

**1 ABSTRACT**

2 This study presents an unsupervised approach for detecting harsh cornering behavior using smartphone-  
3 based telematics enriched with infrastructure data. Unlike traditional methods that require fixed  
4 device orientation or labeled datasets, the proposed framework combines GPS-derived yaw and  
5 heading changes, orientation-invariant inertial sensor magnitudes, and spatial validation using  
6 OpenStreetMap to isolate turning maneuvers with safety relevance. A preprocessing pipeline iden-  
7 tifies candidate turns based on angular thresholds and proximity to mapped intersections. A multi-  
8 variate feature set is extracted from time-series windows around each turn, capturing translational  
9 and rotational dynamics. Outlier detection is performed using DBSCAN, with hyperparameters  
10 tuned via k-distance, and complemented by Isolation Forest to enhance robustness. The ensemble  
11 of detections shows strong separability when evaluated through supervised classifiers, achieving  
12 ROC-AUC scores above 0.98. Visual case studies further confirm the accuracy and interpretability  
13 of the identified events. This orientation-agnostic pipeline operates without labeled data, making  
14 it highly suitable for real-world deployment in driver behavior analysis, risk profiling, and road  
15 safety analytics. The study highlights the feasibility of combining sensor fusion and map-based  
16 filtering to detect unsafe driving behaviors at scale.

17

18 *Keywords:* Smartphone telematics, harsh cornering detection, unsupervised learning, sensor fu-  
19 sion, OpenStreetMap, driver behavior, road safety.

## 1 INTRODUCTION

2 Road safety data sources are essential for understanding the causes of crashes and predicting future  
3 risks to reduce road traffic accidents. Various factors, including driving speed, road infrastructure,  
4 and driver behavior, influence crashes. However, crashes are relatively rare, making it challenging  
5 to detect and assess road safety conditions in real-time. To address this challenge, researchers have  
6 employed crash surrogates in road safety studies in order to define crash proneness and associate  
7 it with crash risk (Gettman et al., Nikolaou et al. (1, 2)).

8 The increasing adoption of smartphone-based telematics offers a scalable and cost-effective  
9 alternative for monitoring driver behavior (Mantouka et al. (3)). Smartphones, equipped with  
10 sensors such as accelerometers, gyroscopes, and GPS, generate rich datasets for analyzing vehicle  
11 dynamics. High G-force events, characterized by vehicle acceleration exceeding expected levels,  
12 typically result from hard braking or abrupt acceleration maneuvers. These events are widely used  
13 by researchers to evaluate driver behavior and identify high-risk drivers (Simons-Morton et al. (4)).

14 Previous studies, such as Liu et al. (5), have explored smartphone-based detection of hard-  
15 braking events to enhance road safety services, demonstrating the potential of mobile sensors in  
16 real-world driving scenarios. Additionally, the use of gyroscopes in mobile applications, as dis-  
17 cussed in Barthold et al. (6), has shown promise in capturing rotational motion, making it a valuable  
18 tool for detecting cornering events.

19 The accurate classification of vehicle cornering behaviors (e.g., normal vs. harsh turns) is  
20 crucial for a wide range of applications, including driver behavior analysis, autonomous driving  
21 systems, and vehicle safety enhancement. Identifying and mitigating harsh driving maneuvers  
22 is particularly significant, as these actions can lead to severe vehicle instability. For example,  
23 while rollover incidents constitute only 3% of all vehicle crashes, they account for nearly one-  
24 third of passenger fatalities, highlighting the critical risks associated with extreme driving events  
25 (Padmanaban and Husher (7)). The ability to detect and analyze these behaviors in real-time could  
26 play a pivotal role in reducing fatalities and improving road safety.

27 While hard braking and rapid acceleration have been extensively studied in the context  
28 of smartphone-based telematics, harsh cornering remains comparatively underexplored despite its  
29 strong association with vehicle instability and elevated crash risk. Most commercial and academic  
30 telematics frameworks focus on longitudinal forces due to their simpler detection using accelerom-  
31 eter data and clearer regulatory implications. However, lateral dynamics during turning are equally  
32 critical, particularly in urban or suburban environments where sharp curves and intersections are  
33 frequent. Cornering events are inherently more complex to capture, as they depend on rotational  
34 motion, trajectory shape, and interaction with road geometry—factors that are difficult to quan-  
35 tify under unknown device orientations. The limited attention given to harsh cornering detection  
36 contrasts with its potential importance in crash prevention, driver feedback, and risk-based in-  
37 surance pricing. This gap highlights the need for robust, orientation-invariant methods capable  
38 of identifying aggressive turning behavior in naturalistic driving conditions. Most existing stud-  
39 ies that investigate harsh cornering rely on smartphones mounted in fixed orientations within the  
40 vehicle, enabling axis-specific thresholding for detecting lateral acceleration or angular velocity  
41 (Vlahogianni and Barmpounakis (8)). Moreover, a few studies rely on special equipment to align  
42 the smartphone to the vehicle’s coordinate system (Wang et al., Chen et al. (9, 10)). While effective  
43 in controlled settings, such methods lack robustness in real-world deployments where the smart-  
44 phone’s position and orientation can vary significantly. To address this limitation, the present study  
45 proposes an unsupervised methodology that leverages smartphone sensor and GPS data fused with

1 infrastructure information from OpenStreetMap. The approach estimates yaw rate over multiple  
 2 temporal horizons to capture the full cornering profile, normalizes inertial data using vector mag-  
 3 nitudes to remain invariant to phone orientation, and filters events based on geospatial validation  
 4 near road intersections. By employing K-NearestNeighbors to guide hyperparameter tuning and  
 5 DBSCAN to identify outliers, harsh cornering events are detected without reliance on labeled data  
 6 or fixed sensor placement. This orientation-agnostic pipeline offers a scalable and flexible solution  
 7 for real-world driving behavior analysis.

## 8 DATA COLLECTION AND PREPROCESSING

9 This section outlines the procedures followed to prepare the data used for detecting harsh cor-  
 10 nering events from smartphone-based telematics. Given the challenges posed by real-world de-  
 11 ployment—such as arbitrary device placement, sensor noise, and inconsistent sampling—careful  
 12 attention was paid to both the selection of meaningful signals and the derivation of robust features.  
 13 The dataset includes multimodal time-series data recorded during naturalistic driving, and prepro-  
 14 cessing steps were designed to extract motion-related cues that can capture turning behavior in a  
 15 device-agnostic manner.

### 16 Data Source

17 The dataset used in this study originates from OSeven Telematics and consists of anonymized  
 18 time-series data collected from smartphone sensors at a frequency of 1 Hz. Each record includes  
 19 GPS-derived location coordinates, speed, and heading (course over ground), as well as readings  
 20 from embedded inertial sensors such as the accelerometer and gyroscope. The data is captured pas-  
 21 sively during driving, leveraging consumer-grade smartphones placed arbitrarily inside the vehicle  
 22 without fixed orientation or mounting. As a result, the dataset reflects realistic deployment con-  
 23 ditions, including variability in device orientation, sensor noise, and driving environments. The  
 24 temporal resolution and multimodal nature of the dataset make it suitable for modeling driving  
 25 behavior and detecting dynamic events such as harsh cornering.

26 In total, the dataset after filtering noisy GPS datapoints comprises 4,017 individual trips  
 27 and 1,758,589 datapoints, representing a large and diverse sample of naturalistic driving behavior  
 28 across various conditions.

### 29 Yaw Rate Estimation

30 To capture turning dynamics, we extract two features: (a) the maximum yaw rate across short hori-  
 31 zons, representing the sharpness of a turn, and (b) the maximum total heading change, representing  
 32 the overall extent of the maneuver. These are derived from GPS-based heading changes sampled  
 33 at 1 Hz.

34 The yaw rate at multiple temporal horizons is computed using Equation (1), which normal-  
 35 izes heading changes over time to account for angular wraparound. The maximum absolute yaw  
 36 rate across the past four seconds is extracted in Equation (2) to capture the sharpest recent change  
 37 in heading. Similarly, the total turn angle at each horizon is defined in Equation (3), and the largest  
 38 absolute heading deviation is summarized in Equation (4). These features together capture both  
 39 the short-term intensity and the spatial extent of vehicle cornering behavior.

$$40 \text{ yaw\_rate}_n = \frac{((\theta_t - \theta_{t-n} + 180) \bmod 360) - 180}{n \cdot \Delta t}, \quad n = 1, 2, 3, 4 \quad (1)$$

$$1 \quad \text{max\_yaw\_rate} = \max(|\text{yaw\_rate}_1|, |\text{yaw\_rate}_2|, |\text{yaw\_rate}_3|, |\text{yaw\_rate}_4|) \quad (2)$$

$$2 \quad \text{turn\_angle}_n = ((\theta_t - \theta_{t-n} + 180) \bmod 360) - 180, \quad n = 1, 2, 3, 4 \quad (3)$$

$$3 \quad \text{max\_turn\_angle} = \max(|\text{turn\_angle}_1|, |\text{turn\_angle}_2|, |\text{turn\_angle}_3|, |\text{turn\_angle}_4|) \quad (4)$$

#### 4 Map-Based Validation Using OpenStreetMap

5 After computing the turn angle at each timestamp, we apply a threshold of 70 degrees over the 4  
 6 seconds period to identify candidate turning events. This threshold is selected to filter out minor  
 7 course deviations and emphasize maneuvers that are likely to affect vehicle stability if executed  
 8 harshly. The resulting candidate events capture high-curvature segments in the trajectory, but they  
 9 may still include false positives due to GPS noise, lane changes, or sudden heading corrections on  
 10 straight roads.

11 To enhance the reliability of turn detection, we introduce a validation step using map data  
 12 from OpenStreetMap (OSM). The key idea is that genuine cornering events should occur in the  
 13 vicinity of an actual road intersection. For each candidate turn event, we query the surrounding  
 14 region within a fixed radius, 15 meters in our case, to check for the presence of an OSM-mapped  
 15 intersection.

16 Intersections are extracted using OSM road network data, typically by identifying nodes  
 17 where multiple road segments meet at an angle, excluding nodes on roundabouts or interchanges.  
 18 If no such intersection is found near the detected turn point, the event is considered a likely false  
 19 positive and is discarded from further analysis.

20 Since the map-based validation is only used to eliminate false positives among the detected  
 21 cornering events, we avoid building a local road graph for each event—which would be computa-  
 22 tionally intensive. Instead, we pre-load and index the entire road network of the Attica region in  
 23 Greece. This area includes a mix of dense urban grids, suburban layouts, and rural roads, offering  
 24 a realistic and structurally diverse environment. By covering this region in advance, we ensure fast  
 25 spatial queries for intersection checks while maintaining robustness across varied road geometries.

26 This spatial filtering step improves precision by enforcing a topological constraint: harsh  
 27 cornering should correspond not just to sharp heading changes, but to those that align with actual  
 28 road geometry. As a result, the dataset used in subsequent modeling stages contains a more robust  
 29 set of turn events grounded in the physical infrastructure of the driving environment.

30 This ensures that the final dataset focuses on significant cornering maneuvers that are more  
 31 likely to impact vehicle stability and driver behavior. Figure 1 illustrates the distribution of total  
 32 turn angles and vehicle speeds across the filtered dataset. As shown, most turns involve angles  
 33 ranging from 70° to 180°, while vehicle speeds during these maneuvers are typically concentrated  
 34 below 40 km/h, consistent with expected driving behavior in urban environments.

35 After validation, the resulting dataset comprises approximately 1,900 high-confidence cor-  
 36 nering events in Attica region of Greece, which form the basis for downstream clustering and  
 37 anomaly detection.

#### 38 Orientation-Invariant Sensor Features

39 Following the map-based validation step, the resulting set of candidate turn events was further pro-  
 40 cessed to extract additional features from the inertial sensors. Given that smartphones in real-world

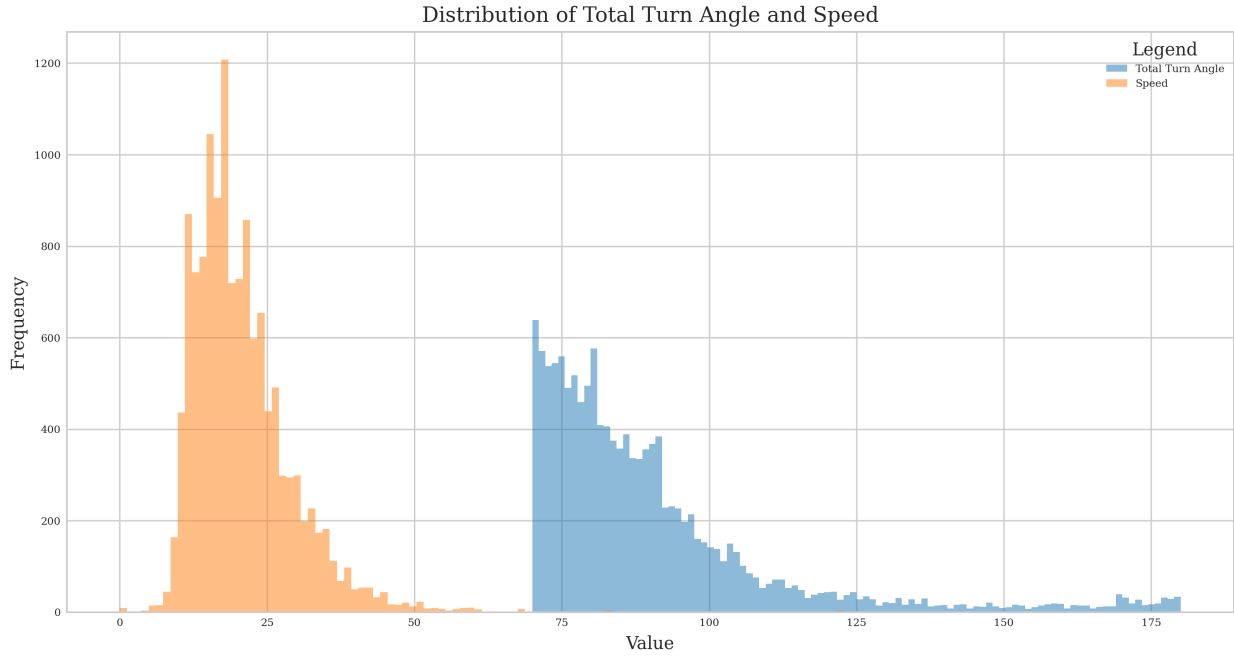


**FIGURE 1:** The histogram shows the distribution of total turn angles (blue) and vehicle speeds (orange) across all turning events in the dataset.

1 deployments can be placed arbitrarily inside the vehicle—resulting in unknown and inconsistent  
 2 orientation—the direct use of individual accelerometer and gyroscope axes (x, y, z) becomes un-  
 3 reliable. To mitigate this, we compute the *magnitude* of the 3-axis accelerometer and gyroscope  
 4 signals, which is invariant to device orientation and better suited for modeling motion intensity.

5 The acceleration and gyroscope magnitude are calculated as the Euclidean norm of the  
 6 three-axis readings at each timestamp  $t$ , as shown in Equations (5), (6):

$$7 \quad \text{accel\_magnitude}_t = \sqrt{a_x(t)^2 + a_y(t)^2 + a_z(t)^2} \quad (5)$$

$$8 \quad \text{gyro\_magnitude}_t = \sqrt{\omega_x(t)^2 + \omega_y(t)^2 + \omega_z(t)^2} \quad (6)$$

9 These magnitude features allow us to quantify the overall intensity of linear and angular  
 10 motion, respectively, without relying on axis-specific orientation. They are particularly useful for  
 11 identifying sudden vehicle dynamics—such as sharp cornering or abrupt lateral shifts—regardless  
 12 of how the phone is positioned within the car.

### 13 **Yaw Rate from Device Orientation Sensors**

14 In addition to estimating yaw rate from GPS-derived heading changes, we also compute a sec-  
 15 ond yaw-related feature using the smartphone’s internal orientation sensor, often referred to as  
 16 motionYaw. This value typically comes from a sensor fusion algorithm that combines data from  
 17 the gyroscope, accelerometer, and magnetometer to provide a stable estimate of the device’s yaw  
 18 (rotation around the vertical axis) relative to the current reference frame.

19 To make this information comparable across time, we calculate the angular velocity—i.e.,  
 20 the yaw rate—by differentiating the motionYaw value over time, taking into account angular

1 wraparound at  $360^\circ$  boundaries. The formula is similar in structure to the GPS-based yaw rate,  
 2 but applied to orientation sensor output:

$$3 \text{ yaw\_rate\_motion}_t = \frac{((\psi_t - \psi_{t-1} + 180) \bmod 360) - 180}{\Delta t} \quad (7)$$

4 where  $\psi_t$  denotes the device yaw angle (in degrees) at time  $t$ , and  $\Delta t$  is the sampling interval.

5 Due to the arbitrary phone placement in real-world scenarios, we use this signal as a sup-  
 6 plementary feature rather than a sole indicator of cornering.

## 7 METHODOLOGY

8 This section describes the full unsupervised pipeline for detecting harsh cornering events from  
 9 smartphone-based telematics. It begins with the construction of time-series segments centered on  
 10 cornering peaks, followed by feature extraction, normalization, and density-based clustering. The  
 11 goal is to identify outlier turn maneuvers that deviate significantly from typical driving behavior.

### 12 Feature Construction

13 Each cornering event identified by the GPS-based turn angle threshold is further processed to ex-  
 14 tract a consistent time-series window for feature computation. Specifically, for each record flagged  
 15 as part of a turn, we identify the *turn peak*—the timestamp where the yaw rate is maximal—and  
 16 extract a 3-second multivariate time-series window centered on this peak.

17 This results in a fixed-length sequence of sensor observations spanning 1 second before  
 18 and 1 second after the peak. Each window includes synchronized values from multiple sensor  
 19 modalities:

- 20 • GPS-derived features: speed, heading
- 21 • Accelerometer: 3-axis linear acceleration
- 22 • Gyroscope: 3-axis angular velocity
- 23 • Device orientation: yaw angle

24 This segmentation process transforms each turn into a comparable multivariate time-series,  
 25 which forms the basis for computing robust, orientation-invariant features.

26 From each time-series segment, we compute a set of 13 statistical and motion-based fea-  
 27 tures that describe the dynamics of the turn. These include speed variations, angular motion inten-  
 28 sities, rotational asymmetry, and trajectory properties. Table 1 summarizes the extracted features.

29 These features collectively encode the intensity, variability, and asymmetry of each cor-  
 30 nering maneuver. By capturing both translational and rotational dynamics—including maximum  
 31 and minimum yaw rates from multiple sources—they offer a rich representation of the vehicle’s  
 32 behavior during turning. The use of magnitudes for inertial sensors ensures robustness to phone  
 33 orientation, while entry/exit speeds and heading change summarize the broader context of each  
 34 maneuver.

### 35 Unsupervised Detection of Harsh Cornering Events

36 After feature extraction, we standardize the feature matrix using z-score normalization, ensuring  
 37 that each feature contributes equally to the distance-based clustering that follows.

38 We then apply the Density-Based Spatial Clustering of Applications with Noise (DB-  
 39 SCAN) algorithm to identify harsh cornering events (Ester et al. (11)). DBSCAN is particularly  
 40 well-suited for this application because it does not require the number of clusters to be specified in  
 41 advance, and it explicitly labels as *noise* those points that do not belong to any dense region.

**TABLE 1:** Description of extracted features for each turn event

Feature	Description
speed_min	Minimum vehicle speed during the turn (km/h)
speed_max	Maximum vehicle speed during the turn (km/h)
entry_speed	Speed at the start of the turn window (km/h)
exit_speed	Speed at the end of the turn window (km/h)
max_speed_change	Maximum speed change observed within the window (km/h)
total_turn_angle_max	Maximum heading change over fixed intervals (degrees)
yaw_rate_max	Max yaw rate computed from GPS heading (°/s)
motion_yaw_rate_deg_max	Max yaw rate from device orientation in degrees/s
motion_yaw_rate_deg_min	Min yaw rate from device orientation in degrees/s
accel_magnitude_min	Minimum acceleration magnitude (m/s <sup>2</sup> )
accel_magnitude_max	Maximum acceleration magnitude (m/s <sup>2</sup> )
gyro_magnitude_min	Minimum gyroscope magnitude (rad/s)
gyro_magnitude_max	Maximum gyroscope magnitude (rad/s)

1 In our setting, this "noise" corresponds to abnormal or harsh turning events, under the  
 2 assumption that most turns follow a typical behavioral pattern. DBSCAN treats these harsh events  
 3 as statistical outliers in the feature space.

#### 4 **Hyperparameter Tuning via K-Distance Heuristic**

5 DBSCAN requires two hyperparameters: the neighborhood radius  $\epsilon$  and the minimum number of  
 6 neighbors (`min_samples`) to form a dense cluster. While `min_samples` is typically set to a fixed  
 7 value, selecting  $\epsilon$  appropriately is crucial for meaningful outlier detection.

8 To identify an appropriate value for the  $\epsilon$  parameter in DBSCAN, we applied the k-distance  
 9 heuristic, plotting the distance to each point's 50th nearest neighbor after sorting all distances in  
 10 ascending order as shown in Figure 2. The resulting curve exhibits a characteristic elbow shape,  
 11 where a steep increase in distance suggests a transition from dense to sparse regions. We selected  
 12 an  $\epsilon$  value of 4.0, which captures the boundary between typical and anomaly turning behaviors.  
 13 This selection balances precision in detecting dense clusters of regular maneuvers and recall in  
 14 identifying true outliers representing harsh cornering.

15 This hybrid approach leverages K-NearestNeighbors to guide DBSCAN parameter tuning  
 16 while maintaining the flexibility of density-based clustering to detect rare but significant behaviors.

17 To assess the internal consistency of clusters formed by DBSCAN, we computed the silhou-  
 18 ette score, a common metric for evaluating unsupervised clustering. The silhouette score quantifies  
 19 how similar each point is to its own cluster compared to other clusters. In our case, DBSCAN  
 20 achieved a silhouette score of 0.53, indicating moderately well-separated clusters, with outliers  
 21 forming distinct, sparse regions in the feature space. This confirms the effectiveness of the ex-  
 22 tracted features and selected  $\epsilon$  in capturing cornering behavior patterns.

23 While unsupervised, this score supports the intuition that regular and harsh cornering events  
 24 occupy distinct zones in the feature space.

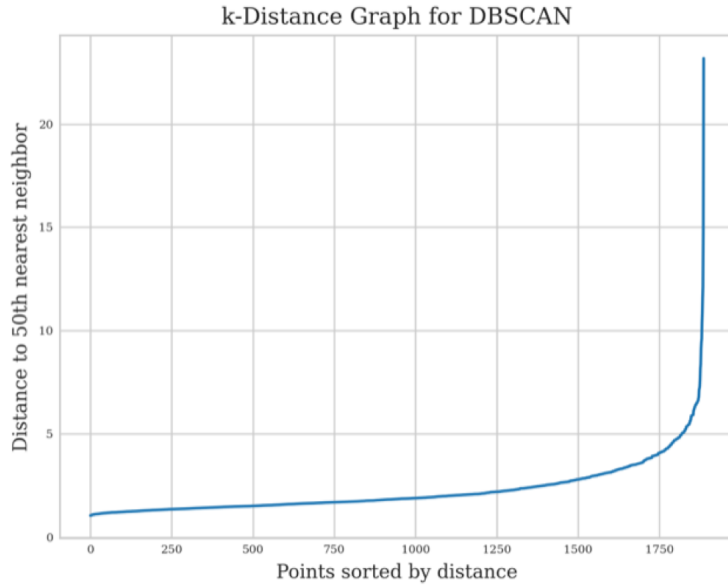


**FIGURE 2:** k-Distance plot used to determine the optimal  $\epsilon$  parameter for DBSCAN. Each point represents the distance to its 50th nearest neighbor, sorted in ascending order

1 **Isolation Forest as a Complementary Detector**

2 In addition to DBSCAN, we evaluated the use of the Isolation Forest algorithm as a model-agnostic  
 3 unsupervised method for detecting anomalous cornering behaviors. Isolation Forest builds an en-  
 4 semble of random binary trees, where anomalous points are isolated with fewer splits. We applied  
 5 the method on the same feature set, using 100 estimators and contamination parameter set to 0.02.  
 6 Events with the shortest average path lengths were flagged as potential harsh turns.

7 To further illustrate the characteristics of the harsh events detected by each method, Figure  
 8 3 presents a comparison of feature distributions between DBSCAN and Isolation Forest detections.  
 9 While both methods show elevated values in yaw-related and inertial features compared to normal  
 10 turns, distinct patterns emerge. DBSCAN-detected events typically exhibit higher turn angles  
 11 and yaw rates, while Isolation Forest tends to flag events with elevated motion asymmetry and  
 12 gyroscope magnitude—even at moderate speeds. These differences support the hypothesis that the  
 13 two methods capture complementary aspects of harsh cornering behavior.

14 Table 2 summarizes the overlap and divergence between DBSCAN and Isolation Forest in  
 15 detecting harsh cornering events. Only 50 harsh corner events were detected by both representing  
 16 nearly 3% of the entire dataset. DBSCAN contributed 22 unique detections, typically involving  
 17 sharp turns with high yaw rates, while Isolation Forest identified 26 distinct events characterized  
 18 by subtle but higher speeds. The complementary nature of these results supports the use of an  
 19 ensemble approach that combines both methods to improve detection robustness.

20 **Validation via Classifier-Based Separability**

21 To assess the internal consistency of the pseudo-labeled harsh cornering events, we evaluated how  
 22 well the extracted features could separate harsh and normal turns using a supervised learning proxy.  
 23 Specifically, we trained two binary classifiers—logistic regression and random forest—using the  
 24 ensemble labels (union of DBSCAN and Isolation Forest detections) as target values.

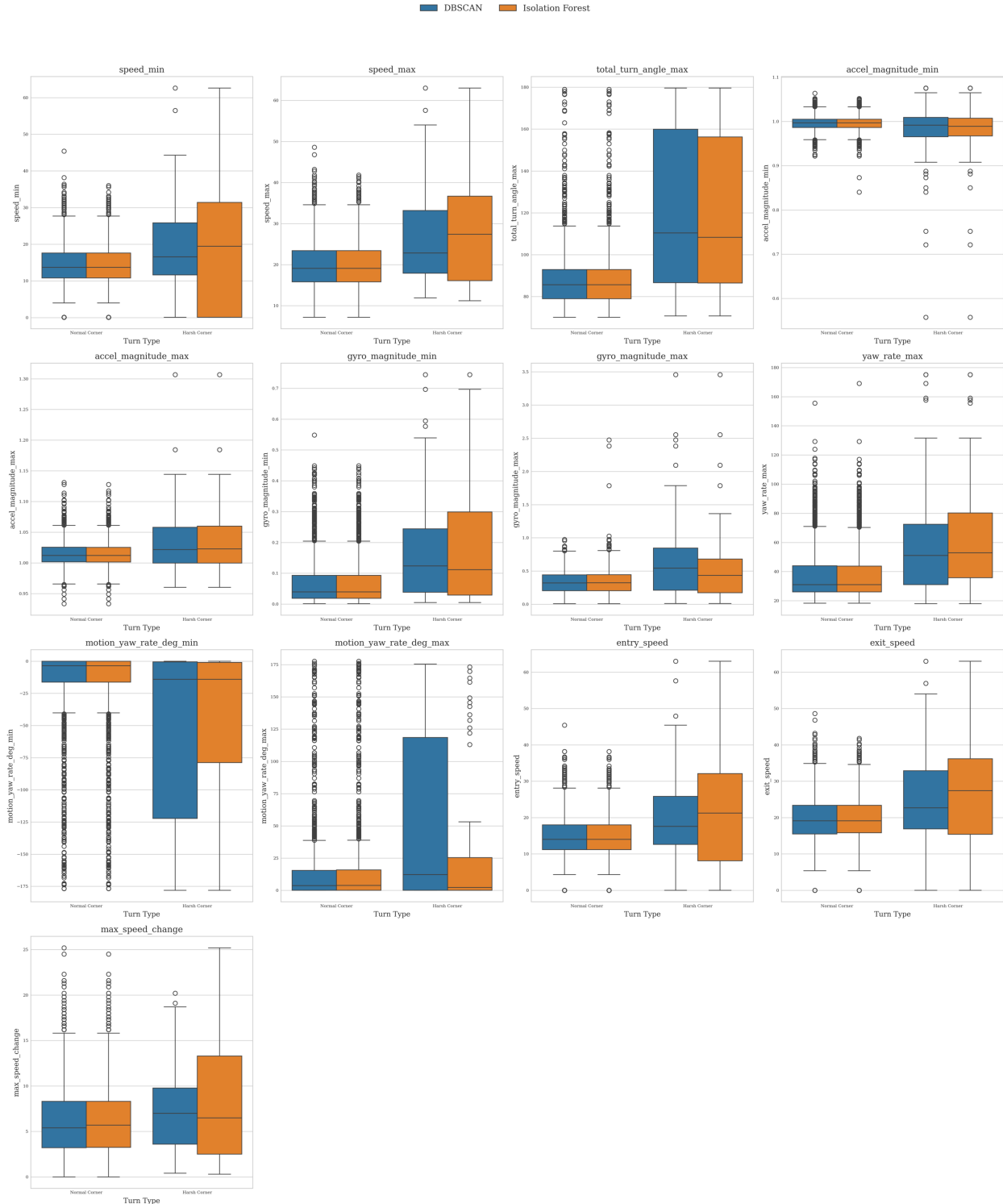


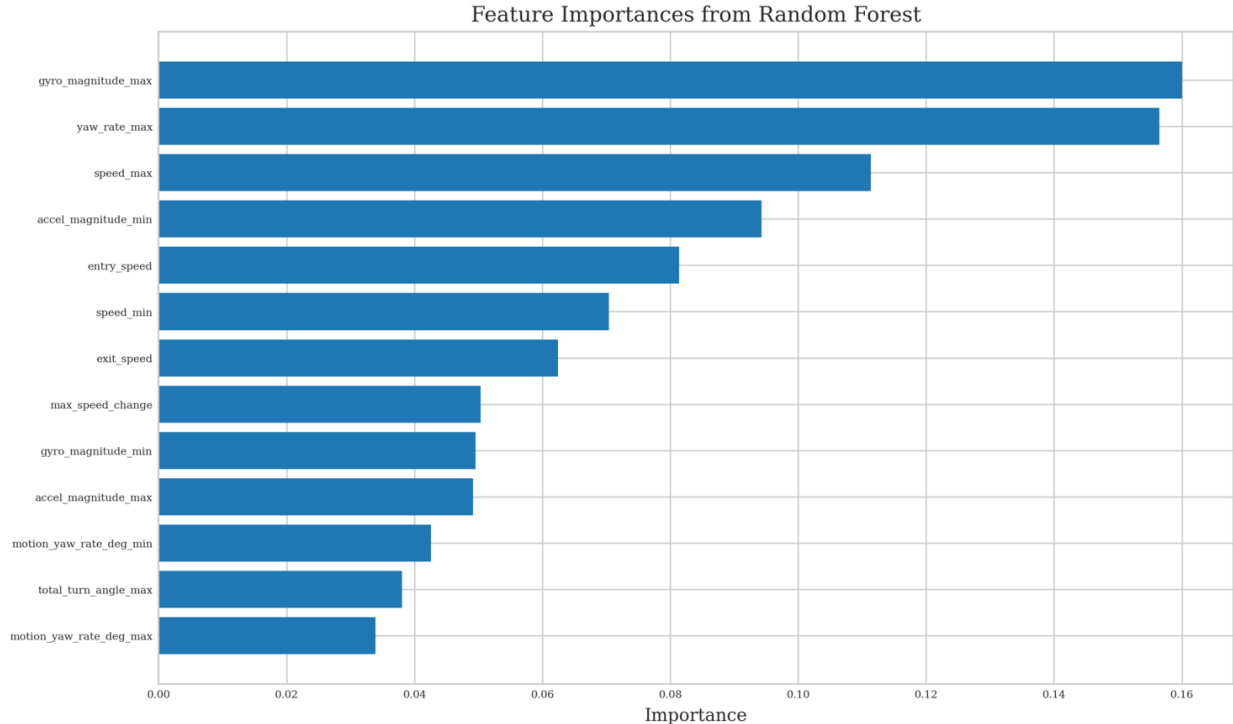
**FIGURE 3:** Comparison of feature distributions for harsh cornering events detected by DBSCAN (blue) and Isolation Forest (orange). Each boxplot represents one of the 13 extracted features, grouped by detection method.

**TABLE 2:** Summary of harsh cornering detections by DBSCAN and Isolation Forest.

Method	Harsh Corners Detected	Unique Events
DBSCAN	72	22
Isolation Forest	76	26
Intersection (Both)	50	-

1 We applied 5-fold cross-validation using ROC-AUC as the evaluation metric. The logistic  
 2 regression model achieved a mean ROC-AUC of  $0.986 \pm 0.007$ , while the random forest classifier  
 3 reached  $0.994 \pm 0.003$ , indicating excellent separability between harsh and normal cornering events  
 4 in the feature space. These results validate that the extracted features—such as yaw rate, turn  
 5 angle, acceleration and gyroscope magnitudes—capture the underlying dynamics of risky turning  
 6 behavior effectively.

7 To further interpret model behavior, we examined feature importances from the random for-  
 8 est model as shown in Figure 4. The most influential features included maximum gyroscope mag-  
 9 nitude, maximum yaw rate and speed confirming their relevance in characterizing high-intensity  
 10 cornering maneuvers. These findings support the validity of the unsupervised ensemble detec-  
 11 tion pipeline and highlight the robustness of the feature design in distinguishing abnormal vehicle  
 12 dynamics.

**FIGURE 4:** Feature importance scores from the random forest classifier trained to separate harsh vs. normal cornering events using ensemble labels.

## 1 Qualitative Case Studies and Map-Based Validation

2 To complement the quantitative validation, we performed qualitative case studies by visualizing  
3 predicted harsh cornering events on real-world GPS trajectories. Using the original time-series  
4 data, we plotted the location of each detected event on a digital map.

5 Figure 5 illustrates several representative examples of harsh cornering maneuvers detected  
6 by the ensemble model. For each case, we annotated the turn location with always-visible labels  
7 indicating vehicle speed and yaw rate. The trajectories clearly show sharp changes in direction or  
8 dynamics consistent with risky maneuvers. These visualizations confirm that the detected events  
9 correspond to turning behavior, and reinforce the effectiveness of combining orientation-invariant  
10 features, map-based filtering, and outlier detection.

11 These case studies further support the model’s real-world interpretability and its potential  
12 applicability in driver feedback systems, road safety analytics, and fleet risk profiling.

13 Figure 5a depicts a harsh cornering event at an urban intersection, where the vehicle enters  
14 the turn at a high speed of 42km/h—substantially exceeding typical safe turning speeds in such en-  
15 vironments. In Figure 5b, the vehicle executes a moderately fast cornering maneuver, with speeds  
16 ranging from 21 to 27km/h and yaw rates up to 27.4°/s, indicative of assertive but not necessarily  
17 unsafe driving. Figure 5c captures a sharp turn initiated immediately after departure, where the  
18 vehicle accelerates from 0 to 12km/h while reaching a peak yaw rate of 80°/s. This combination of  
19 low speed and extremely high angular velocity suggests a potentially unstable or abrupt maneuver.  
20 Lastly, Figure 5d presents a harsh 90° intersection turn with sustained high yaw rates, peaking at  
21 47.5°/s. The vehicle performs the turn at speeds between 18 and 23 km/h, reflecting a tight and  
22 aggressive maneuver that may compromise stability in a confined urban setting.

## 23 DISCUSSION

### 24 Summary of Key Findings

25 This study developed and evaluated a fully unsupervised framework for detecting harsh cornering  
26 behavior using smartphone-based telematics and infrastructure data. By extracting yaw and turn  
27 dynamics from GPS, aggregating orientation-invariant inertial features, and validating events spa-  
28 tially with OpenStreetMap, the methodology identifies high-risk maneuvers in naturalistic driving  
29 conditions. Unsupervised clustering with DBSCAN and Isolation Forest allowed for robust detec-  
30 tion without the need for ground truth labels or fixed device mounting. The detected events showed  
31 strong separability in feature space, and qualitative map visualizations confirmed their real-world  
32 plausibility, demonstrating the strength of the approach in capturing aggressive turning patterns at  
33 scale.

### 34 Limitations

35 Despite the promising results, the study has several limitations that inform both the scope of inter-  
36 pretation and future development. One key limitation lies in the temporal resolution of GPS data.  
37 Sampling at 1 Hz restricts the granularity of yaw rate estimation and may fail to fully capture the  
38 sharpness of brief, high-intensity turns, especially in fast-moving traffic scenarios. Additionally,  
39 the lack of labeled ground truth data precludes formal validation of detection precision or recall.  
40 Although proxy evaluations using supervised classifiers and qualitative visual inspection support  
41 the method’s internal consistency, direct confirmation through video annotations or expert reviews  
42 would offer stronger validation.

43 Another constraint arises from the geographical specificity of the dataset. Since the data



**FIGURE 5:** Representative examples of detected harsh cornering events visualized on real-world map trajectories. Red markers indicate turning peaks, annotated with speed and yaw rate.

- 1 predominantly represents urban driving in Greece, the model may not generalize equally well
- 2 across countries, climates, or vehicle types. Differences in road layout, driving culture, and smart-
- 3 phone sensor characteristics could affect the reliability of feature patterns and detection thresholds.

1 The reliance on sensor magnitudes to maintain orientation invariance also removes directional con-  
2 text, which could be useful for more granular behavioral profiling or risk assessment. Lastly, the  
3 use of OpenStreetMap for validating turns assumes high-quality and up-to-date map data, which  
4 may not hold true in all regions, potentially reducing the applicability of the method in poorly  
5 mapped areas.

## 6 **Practical Applications**

7 Despite these limitations, the proposed framework has significant potential for real-world appli-  
8 cation across several domains. In driver behavior analysis and usage-based insurance, the ability  
9 to detect harsh cornering events without requiring sensor calibration or labeled data makes the  
10 pipeline well-suited for large-scale deployment on consumer smartphones. It can serve as a basis  
11 for driver risk scoring, performance feedback, or targeted coaching interventions. Fleet opera-  
12 tors could use the system to monitor aggressive maneuvers and prevent vehicle wear, while also  
13 improving safety outcomes across their networks.

14 Moreover, road safety agencies and urban planners could benefit from spatially aggregating  
15 harsh cornering detections to identify risky intersections or infrastructure gaps. Such data-driven  
16 insights could support decision-making for traffic calming measures or redesigns. Finally, the  
17 mobile-friendly nature of the approach lends itself to real-time use in driver assistance systems or  
18 mobility apps, enabling live feedback during trip execution and promoting safer driving habits over  
19 time.

20 Furthermore, the proposed framework can be extended by introducing a severity scoring  
21 system for detected harsh cornering events. By aggregating normalized values of yaw rate, turn an-  
22 gle, and gyroscopic magnitude into a composite severity index, each detected event can be ranked  
23 on a continuous scale rather than as a binary classification. This enables more nuanced interpreta-  
24 tions of driver behavior and supports stratified feedback mechanisms, where different intervention  
25 levels are matched to the severity of the maneuver. Severity scoring can also assist insurers in  
26 dynamically adjusting driver risk scores based on cumulative event intensity over time, rather than  
27 event frequency alone.

## 28 **Future Research Directions**

29 Several extensions could further improve the methodology and expand its scope. One avenue is  
30 the integration of complementary data sources, such as dashcam video or environmental and in-  
31 frastructure context, to enhance interpretability and aid in severity classification. Employing self-  
32 supervised or contrastive learning could unlock richer representations from large unlabeled datasets  
33 and improve cross-device generalization. Additionally, introducing directional features—perhaps  
34 through soft alignment with vehicle motion or inferred device orientation—could bring back val-  
35 uable information without losing robustness.

36 Personalization of detection thresholds based on individual driving baselines may further  
37 enhance sensitivity and relevance, particularly when combined with privacy-preserving technolo-  
38 gies like federated learning.

39 Finally, deploying the pipeline in real-time on mobile devices or edge platforms would al-  
40 low for instant detection and feedback, enabling new applications in connected vehicle systems and  
41 behavioral safety platforms. Moreover, aggregating detected events across space and time could  
42 support the creation of road safety heatmaps, helping identify high-risk locations and informing  
43 infrastructure improvements or targeted traffic interventions.

**1 CONCLUSIONS**

2 This work presents a novel, unsupervised, and orientation-invariant approach to detecting harsh  
3 cornering behavior using standard smartphone sensors and open-source map data. The proposed  
4 pipeline successfully circumvents the limitations of fixed sensor placement and labeled training  
5 data, instead relying on outlier detection in a multi-sensor feature space to isolate aggressive  
6 turning events. By validating candidate maneuvers against real road geometry and demonstrating  
7 strong internal consistency in the resulting detections, the framework proves suitable for real-world  
8 driving behavior analysis.

9 The method's flexibility, low deployment cost, and robustness to phone placement make  
10 it highly applicable to modern telematics systems, driver monitoring solutions, and safety intelli-  
11 gence platforms. While limitations related to sampling rate, contextual generalization, and ground  
12 truth remain, the study establishes a strong foundation for unsupervised behavioral detection in  
13 naturalistic settings. As smartphone sensing and computational capabilities continue to improve,  
14 the proposed approach stands to play a significant role in advancing data-driven road safety and  
15 personalized mobility technologies.

**16 ACKNOWLEDGEMENTS**

17 This research has been conducted within the IVORY project. The project has received funding from  
18 the European Union's Horizon Europe research and innovation programme under grant agreement  
19 No 101119590.

1 **REFERENCES**

- 2 1. Gettman, D. M., L. Pu, T. Sayed, and S. G. Shelby, Surrogate Safety Assessment Model  
3 and Validation: Final Report, 2008.
- 4 2. Nikolaou, D., A. Ziakopoulos, and G. Yannis, A Review of Surrogate Safety Measures  
5 Uses in Historical Crash Investigations. *Sustainability*, Vol. 15, No. 9, 2023.
- 6 3. Mantouka, E., M. Barmpounakis, E. Vlahogianni, and J. Golias, Smartphone Sensing for  
7 Understanding Driving Behavior: Current Practice and Challenges. *International Journal  
8 of Transportation Science and Technology*, Vol. 10, 2020.
- 9 4. Simons-Morton, B., K. Cheon, F. Guo, and P. Albert, Trajectories of Kinematic Risky  
10 Driving Among Novice Teenagers. *Accident; analysis and prevention*, Vol. 51C, 2012, pp.  
11 27–32.
- 12 5. Liu, L., D. Racz, K. Vaillancourt, J. Michelman, M. Barnes, S. Mellem, P. Eastham,  
13 B. Green, C. Armstrong, R. Bal, S. O'Banion, and F. Guo, *Smartphone-based Hard-  
14 braking Event Detection at Scale for Road Safety Services*, 2022.
- 15 6. Barthold, C., K. Pathapati Subbu, and R. Dantu, Evaluation of gyroscope-embedded mo-  
16 bile phones. In *2011 IEEE International Conference on Systems, Man, and Cybernetics*,  
17 2011, pp. 1632–1638.
- 18 7. Padmanaban, J. and S. Husher, Occupant injury experience in rollover crashes: an in-  
19 depth review of NASS/CDS data. *Annu Proc Assoc Adv Automot Med*, Vol. 49, 2005, pp.  
20 103–118.
- 21 8. Vlahogianni, E. I. and E. N. Barmpounakis, Driving analytics using smartphones: Algo-  
22 rithms, comparisons and challenges. *Transportation Research Part C: Emerging Technolo-  
23 gies*, Vol. 79, 2017, pp. 196–206.
- 24 9. Wang, Y., Y. Chen, J. Yang, M. Gruteser, R. Martin, H. Liu, L. Liu, and Karataş, Determin-  
25 ing Driver Phone Use by Exploiting Smartphone Integrated Sensors. *IEEE Transactions  
26 on Mobile Computing*, Vol. 15, 2015, pp. 1–1.
- 27 10. Chen, D., K.-T. Cho, S. Han, Z. Jin, and K. Shin, Invisible Sensing of Vehicle Steering  
28 with Smartphones, 2015, pp. 1–13.
- 29 11. Ester, M., H.-P. Kriegel, J. Sander, and X. Xu, A Density-Based Algorithm for Discovering  
30 Clusters in Large Spatial Databases with Noise. In *Knowledge Discovery and Data Mining*,  
31 1996.